

Molecular states $J/\psi B_c^+$ and $\eta_c B_c^{*+}$

S. S. Agaev,¹ K. Azizi,^{2,3,*} and H. Sundu⁴

¹*Institute for Physical Problems, Baku State University, Az-1148 Baku, Azerbaijan*

²*Department of Physics, University of Tehran, North Karegar Avenue, Tehran 14395-547, Iran*

³*Department of Physics, Dogus University, Dudullu-Ümraniye, 34775 Istanbul, Türkiye*

⁴*Department of Physics Engineering, Istanbul Medeniyet University, 34700 Istanbul, Türkiye*

(ΩDated: April 30, 2026)

Hadronic molecules $\mathfrak{M} = J/\psi B_c^+$ and $\widetilde{\mathfrak{M}} = \eta_c B_c^{*+}$ are investigated in the framework of QCD sum rule method. These particles with spin-parities $J^P = 1^+$ have the quark contents $c\bar{c}\bar{b}$. We compute their masses and current couplings and find that they are numerically very close to each other coinciding within accuracy of the sum rule method. Therefore, we concentrate on the molecule $J/\psi B_c^+$ and explore features of this state in a detailed form. Our prediction $m = (9740 \pm 70)$ MeV for its mass means that \mathfrak{M} easily decays to pairs of ordinary mesons through strong interactions. There are two mechanisms responsible for transformations of \mathfrak{M} to conventional mesons. The fall-apart mechanism generates the dominant decay channels $\mathfrak{M} \rightarrow J/\psi B_c^+$ and $\mathfrak{M} \rightarrow \eta_c B_c^{*+}$. Annihilation of $\bar{c}c$ quarks triggers subdominant processes with various final-state B and D mesons: Six of such channels are considered in this work. The partial widths all of decays are computed using the three-point sum rule approach. The width $\Gamma[\mathfrak{M}] = (121 \pm 17)$ MeV of the hadronic axial-vector molecule \mathfrak{M} , as well as its mass provide valuable information for running and future experiments.

I. INTRODUCTION

Hadronic molecules built of conventional meson pairs are interesting objects and deserve detailed studies within framework of high energy physics. Such molecules may be composed of two mesons and contain four quarks of the same or different flavors. Because existence of such systems, as well as ones with diquark-antidiquark organization, does not contradict to principles of the Quantum Chromodynamics (QCD), their theoretical and experimental analyses are among priorities of the hadron physics.

Suggestions to consider some of resonances observed in experiments as bound/resonant states of conventional mesons were made fifty years ago [1–3]. Thus, it was supposed to interpret numerous vector states discovered in e^+e^- annihilations as structures composed of D meson pairs. These hypothetical molecules contain both the heavy and light quarks.

In the years since, theoretical studies led to advancing the idea of hadronic molecules. Now information collected on parameters of numerous hadronic molecules, on their binding, production and decay mechanisms forms rather strong basis for running and future experiments. This theoretical activity was accompanied by elaborating of new and adapting existing methods and models for investigations of hadronic molecular states. Last publications and references therein give one a better understanding of achievements made in this growing area of the hadron physics [4–16].

Fully heavy hadronic molecules, i.e., molecules composed of heavy mesons and containing only b and c quarks are relatively new states attracted interests due to recent LHCb-CMS-ATLAS discoveries of X structures [17–19]. These presumably exotic $c\bar{c}\bar{c}$ mesons were investigated by employing different approaches. The diquark-antidiquark and hadronic molecule pictures are mostly utilized models to describe properties of these states. Relevant problems were also addressed in our articles Refs. [20, 21], in which we computed parameters of the molecules $\eta_c \eta_c$, $\chi_{c0} \chi_{c0}$, and $\chi_{c1} \chi_{c1}$ and interpreted some of them as candidates to X structures.

The heavy charm-bottom molecules built of equal number of b and c quarks were examined in different papers [7, 15, 16, 22–24]. The coupled-channel unitary approach was applied in Ref. [15] to study states $B_c^{(*)+} B_c^{(*)-}$. The parameters of such molecules with $J^{PC} = 0^{++}$, 1^{++} , and 2^{++} were calculated in our works [22–24]. We performed corresponding analyses using the QCD sum rule (SR) method, which allows one to evaluate parameters of ordinary and exotic hadrons [25–28]. In this approach we find the mass $m \pm \delta m$ of a particle with the central value m and ambiguities $\pm \delta m$ emerged during these computations. In other words, the region $[m - \delta m, m + \delta m]$ can be used to fix the mass of a particle of interest.

*Corresponding Author

The fully heavy asymmetric molecules with contents $bb\bar{c}$ and $cc\bar{b}$ were explored in the literature [16, 29, 30] as well. In Refs. [29, 30] the scalar $\mathcal{M}_b = \eta_b B_c^-$ and $\mathcal{M}_c = \eta_c B_c^+$, and axial-vector $\mathcal{M}_{AV} = \Upsilon B_c^-$ [$\widetilde{\mathcal{M}}_{AV} = \eta_b B_c^{*+}$] structures were studied using the SR method, where we computed the masses and decay widths of these structures. The molecules with a prevalence of b -quarks are close to corresponding two-meson thresholds provided one uses for analysis the central value m . In this scenario, both the scalar \mathcal{M}_b and axial-vector \mathcal{M}_{AV} molecules are resonant states and dissociate to constituent mesons. In the lower limit of the masses, i.e., in a situation when $m - \delta m$, the molecules \mathcal{M}_b and \mathcal{M}_{AV} reside below two-meson thresholds and form bound structures. This means that they cannot decay to mesons which are their ingredients, or decay to particles which contain all four initial quarks. Nevertheless, \mathcal{M}_b and \mathcal{M}_{AV} transform to ordinary mesons through strong processes which occur due to annihilation of $b\bar{b}$ quarks into light $q\bar{q}$ and $s\bar{s}$ pairs followed by creations of ordinary mesons [31–33]. Thus, there are two mechanisms for transformation of four-quark hadronic molecules to ordinary particles. In our previous works [29, 30] we used both of these mechanisms to evaluate total widths of the hadronic molecules $\eta_b B_c^-$ and ΥB_c^- .

In the case of the scalar molecule $\mathcal{M}_c = \eta_c B_c^+$ this scenario changes qualitatively. It turns out that the molecule \mathcal{M}_c dissociates to its components $\eta_c + B_c^+$ even in the lower value of its mass. Hence, it does not form a bound state in a sense emphasized above.

In present work, we study the axial-vector counterparts of \mathcal{M}_c , i.e., consider the molecules $\mathfrak{M} = J/\psi B_c^+$ and $\widetilde{\mathfrak{M}} = \eta_c B_c^{*+}$ built of $cc\bar{b}$ quarks. It is evident that these quarks may be grouped into two different colorless components—ordinary heavy mesons. Thus, \mathfrak{M} is a system of the vector charmonium J/ψ and pseudoscalar B_c^+ meson, whereas $\widetilde{\mathfrak{M}}$ contains the pseudoscalar charmonium η_c and vector meson B_c^{*+} . We are going to compute the masses and decay widths of \mathfrak{M} and $\widetilde{\mathfrak{M}}$ in the framework of QCD SR method. We find that whilst \mathfrak{M} and $\widetilde{\mathfrak{M}}$ have different internal organizations and are different molecules, their masses and current couplings are numerically very close each other. They have identical quark contents and quantum numbers, as a result, their decay patterns do not differ from each other as well. Because the SR method leads to predictions with some uncertainties, we cannot clearly distinguish these structures. Therefore, in this work we concentrate on properties of the molecule \mathfrak{M} .

To this end, apart from the mass and current coupling, we address also various decay channels of the molecule \mathfrak{M} . It is strong-interaction unstable state and decays to ordinary meson pairs through two mechanisms discussed just above. The processes $\mathfrak{M} \rightarrow J/\psi B_c^+$ and $\eta_c B_c^{*+}$ are dominant decay modes of the molecule \mathfrak{M} . The second mechanism gives rise to subdominant channels $\mathfrak{M} \rightarrow B^{*+} D^0$, $B^{*0} D^+$, $B^+ D^{*0}$, $B^0 D^{*+}$, $B_s^{*0} D_s^+$, and $B_s^0 D_s^{*+}$ which belong to this category of processes.

To evaluate the partial widths all of aforementioned decays, we invoke technical tools of the three-point SR method necessary to find strong couplings at corresponding \mathfrak{M} -meson-meson vertices. When exploring the annihilation channels we employ also a relation between heavy quark vacuum expectation value $\langle \bar{c}c \rangle$ and gluon condensate $\langle \alpha_s G^2/\pi \rangle$. But this manipulation does lead to additional free parameters in analysis.

This article is organized in the following way: The masses and current couplings of the hadronic molecules $J/\psi B_c^+$ and $\eta_c B_c^{*+}$ are calculated in Sec. II. In Sec. III we consider the decay channels $\mathfrak{M} \rightarrow J/\psi B_c^+$ and $\eta_c B_c^{*+}$ and calculate their partial widths. The subdominant modes of \mathfrak{M} are explored in Secs. IV and V. In section V we present our prediction for the full decay width of the molecule $J/\psi B_c^+$. The last part, VI, of this paper is reserved for discussion and contains also our concluding remarks.

II. MASSES AND CURRENT COUPLINGS OF THE MOLECULES $J/\psi B_c^+$ AND $\eta_c B_c^{*+}$

To find the spectroscopic parameters of the hadronic molecules $J/\psi B_c^+$ and $\eta_c B_c^{*+}$, one should start form analysis of the correlator

$$\Pi_{\mu\nu}(p) = i \int d^4x e^{ipx} \langle 0 | \mathcal{T} \{ I_\mu(x) I_\nu^\dagger(0) \} | 0 \rangle, \quad (1)$$

where $I_\mu(x)$ [$\widetilde{I}_\mu(x)$] is the interpolating current for the molecule \mathfrak{M} ($\widetilde{\mathfrak{M}}$), while \mathcal{T} is the time-ordered product of currents. The current $I_\mu(x)$ has the following form

$$I_\mu(x) = \bar{c}_a(x) \gamma_\mu c_a(x) \bar{b}_b(x) i \gamma_5 c_b(x). \quad (2)$$

In the case of the structure $\widetilde{\mathfrak{M}}$, we employ the current

$$\widetilde{I}_\mu(x) = \bar{c}_a(x) i \gamma_5 c_a(x) \bar{b}_b(x) \gamma_\mu c_b(x), \quad (3)$$

and calculate the correlator $\widetilde{\Pi}_{\mu\nu}(p)$ obtained from Eq. (1) after substitution $I_\mu(x) \rightarrow \widetilde{I}_\mu(x)$. In these currents $b(x)$ and $c(x)$ are the heavy quark fields with color indices a and b .

To find sum rules for the mass m and current coupling Λ of \mathfrak{M} one has to calculate the correlation function $\Pi_{\mu\nu}(p)$ using two different approaches. First, it should be expressed in terms of the parameters m and Λ , which establishes the phenomenological component $\Pi_{\mu\nu}^{\text{Phys}}(p)$ of the relevant SRs. The correlation function $\Pi_{\mu\nu}^{\text{Phys}}(p)$ is given by the formula

$$\Pi_{\mu\nu}^{\text{Phys}}(p) = \frac{\langle 0|I_\mu|\mathfrak{M}(p, \epsilon)\rangle\langle\mathfrak{M}(p, \epsilon)|I_\nu^\dagger|0\rangle}{m^2 - p^2} + \dots, \quad (4)$$

with ϵ_μ being the polarization vector of the axial-vector state \mathfrak{M} . We write only down the contribution of the ground-state molecule, while the dots stand for contributions of the higher resonances and continuum states.

To compute $\Pi_{\mu\nu}^{\text{Phys}}(p)$ we make use of the matrix element

$$\langle 0|I_\mu|\mathfrak{M}(p, \epsilon)\rangle = \Lambda\epsilon_\mu(p), \quad (5)$$

and get

$$\Pi_{\mu\nu}^{\text{Phys}}(p) = \frac{\Lambda^2}{m^2 - p^2} \left(g_{\mu\nu} - \frac{p_\mu p_\nu}{m^2} \right) + \dots. \quad (6)$$

The correlator $\Pi_{\mu\nu}(p)$ has to be found in terms of the heavy quark propagators $S_{b(c)}(x)$ (see, Ref. [28]) and calculated by applying the techniques of the operator product expansion (OPE). For $\Pi_{\mu\nu}^{\text{OPE}}(p)$, we obtain

$$\begin{aligned} \Pi_{\mu\nu}^{\text{OPE}}(p) = & i \int d^4x e^{ipx} \text{Tr} \left\{ \left[\gamma_\mu S_c^{ab'}(x) \gamma_5 S_b^{b'b}(-x) \gamma_5 S_c^{ba'}(x) \gamma_\nu S_c^{a'a}(-x) \right] \right. \\ & \left. - \text{Tr} \left[\gamma_\mu S_c^{aa'}(x) \gamma_\nu S_c^{a'a}(-x) \right] \text{Tr} \left[\gamma_5 S_c^{bb'}(x) \gamma_5 S_b^{b'b}(-x) \right] \right\}, \end{aligned} \quad (7)$$

which is the QCD side of the sum rules.

The correlation functions $\Pi_{\mu\nu}^{\text{Phys}}(p)$ and $\Pi_{\mu\nu}^{\text{OPE}}(p)$ are composed of two Lorentz structures. The terms $\sim g_{\mu\nu}$ in these correlators are formed due to contributions of the spin-1 particle, therefore are suitable for SR analysis. We denote by $\Pi^{\text{Phys}}(p^2)$ and $\Pi^{\text{OPE}}(p^2)$ corresponding invariant amplitudes. In the case of $\Pi_{\mu\nu}^{\text{Phys}}(p)$ this amplitude is equal to $\Pi^{\text{Phys}}(p^2) = \Lambda^2/(m^2 - p^2)$.

Having equated $\Pi^{\text{Phys}}(p^2)$ and $\Pi^{\text{OPE}}(p^2)$, performed required manipulations (see, for instance, Ref. [34]), we derive SRs for the mass m and current coupling Λ of the molecule \mathfrak{M}

$$m^2 = \frac{\Pi'(M^2, s_0)}{\Pi(M^2, s_0)}, \quad (8)$$

and

$$\Lambda^2 = e^{m^2/M^2} \Pi(M^2, s_0). \quad (9)$$

In Eqs. (8) and (9) $\Pi(M^2, s_0)$ is the amplitude $\Pi^{\text{OPE}}(p^2)$ after the Borel transformation and continuum subtraction, and $\Pi'(M^2, s_0) = d\Pi(M^2, s_0)/d(-1/M^2)$. The Borel transformation is applied to suppress contributions of higher resonances and continuum states, while using the continuum subtraction we remove them from the QCD side of the SR equality.

These manipulations generates a dependence of $\Pi(M^2, s_0)$ on the Borel M^2 and continuum subtraction s_0 parameters. It is given by the expression

$$\Pi(M^2, s_0) = \int_{(3m_c+m_b)^2}^{s_0} ds \rho^{\text{OPE}}(s) e^{-s/M^2} + \Pi(M^2), \quad (10)$$

where $\rho^{\text{OPE}}(s)$ is the spectral density which is equal to an imaginary part of $\Pi^{\text{OPE}}(p^2)$. Because we take into account contributions to $\Pi^{\text{OPE}}(p^2)$ arising from the perturbative and terms proportional to $\langle\alpha_s G^2/\pi\rangle$, $\rho^{\text{OPE}}(s)$ is a sum of the components $\rho^{\text{pert.}}(s)$ and $\rho^{\text{Dim4}}(s)$. The function $\Pi(M^2)$ does not contain contributions included into $\rho^{\text{OPE}}(s)$ and is derived from the correlation function $\Pi^{\text{OPE}}(p)$.

To start numerical computations we fix the gluon condensate $\langle\alpha_s G^2/\pi\rangle = (0.012 \pm 0.004) \text{ GeV}^4$ and masses $m_c = (1.2730 \pm 0.0046) \text{ GeV}$ and $m_b = (4.183 \pm 0.007) \text{ GeV}$ of the quarks which are universal quantities [25, 26, 35]. The parameters M^2 and s_0 depend on a considering process and have to satisfy usual constraints of SR studies. The prevalence of the pole contribution (PC) in extracted quantities is one of such important restrictions. Therefore,

we choose M^2 and s_0 in such a way that to ensure $PC \geq 0.5$. The next constraint is convergence of the operator product expansion. We calculate $\Pi(M^2, s_0)$ by taking into account dimension-4 nonperturbative terms, therefore require fulfillment of $|\Pi^{\text{Dim4}}(M^2, s_0)| \leq 0.05|\Pi(M^2, s_0)|$ which is sufficient for convergence of OPE. Additionally, physical parameters of \mathfrak{M} have to be stable upon variations of M^2 and s_0 .

We have conducted numerical analysis of m and Λ using broad windows for the parameters M^2 and s_0 . Information gathered during these computations has permitted us to restrict limits of M^2 and s_0

$$M^2 \in [8, 10] \text{ GeV}^2, \quad s_0 \in [109, 111] \text{ GeV}^2, \quad (11)$$

where all aforementioned constraints are satisfied. Thus, the s_0 -averaged PC at $M^2 = 10 \text{ GeV}^2$ is equal to 0.52, meanwhile at $M^2 = 8 \text{ GeV}^2$ it amounts to 0.78. At $M^2 = 8 \text{ GeV}^2$ the term $\Pi^{\text{Dim4}}(M^2, s_0)$ and does not exceed 2% of $\Pi(M^2, s_0)$. Dependence of the pole contribution on M^2 is plotted in Fig. 1.

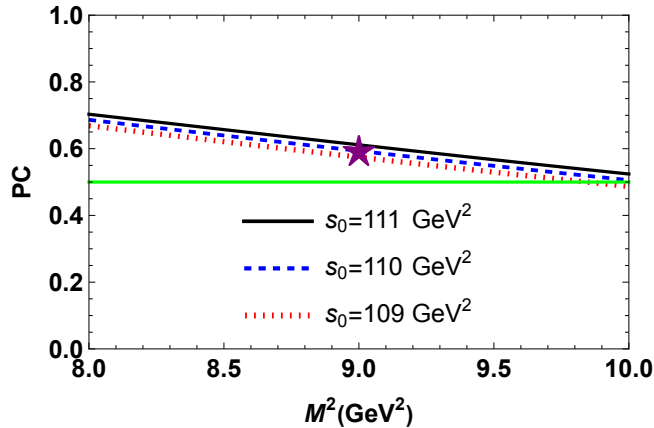


FIG. 1: PC as a function of the Borel parameter M^2 at fixed s_0 . The star shows the point $M^2 = 9 \text{ GeV}^2$, $s_0 = 110 \text{ GeV}^2$.

The parameters m and Λ extracted using SRs and regions Eq. (11) are equal to

$$m = (9740 \pm 70) \text{ MeV}, \quad \Lambda = (5.19 \pm 0.49) \times 10^{-1} \text{ GeV}^5. \quad (12)$$

Ambiguities in Eq. (12) amount to $\pm 0.7\%$ for m , and to $\pm 9.5\%$ in the case of the parameter Λ . They are mostly connected with the choice M^2 and s_0 . The masses of quarks and gluon condensate also contains errors, but their effects on the results are negligible. It is worth noting that uncertainties in Eq. (12) are acceptable for SR computations. The mass m as a function of M^2 and s_0 is depicted in Fig. 2. One sees that lines presented in this figure are stable (within existing errors) upon variations of the parameters M^2 and s_0 .

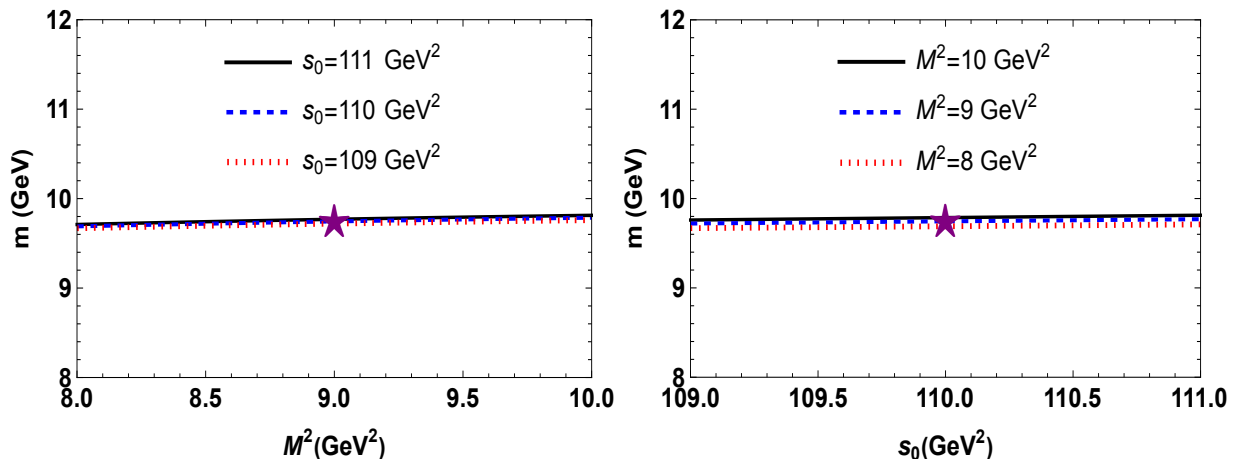


FIG. 2: Dependence of m on the parameters M^2 (left panel), and s_0 (right panel).

The spectroscopic parameters \tilde{m} and $\tilde{\Lambda}$ of the molecule $\tilde{\mathfrak{M}}$ are calculated in accordance with a scheme described above. Computations lead to the following predictions

$$\tilde{m} = (9737 \pm 71) \text{ MeV}, \quad \tilde{\Lambda} = (5.23 \pm 0.50) \times 10^{-1} \text{ GeV}^5. \quad (13)$$

It is clear that these parameters are very close to ones written down in Eq. (12): There are wide overlapping regions for m , Λ and \tilde{m} , $\tilde{\Lambda}$. Because theoretical errors do not allow us to distinguish clearly the states \mathfrak{M} and $\tilde{\mathfrak{M}}$, in what follows, we explore the molecule \mathfrak{M} .

III. DOMINANT DECAY CHANNELS

This section is devoted to analysis of the dominant decays $\mathfrak{M} \rightarrow J/\psi B_c^+$ and $\mathfrak{M} \rightarrow \eta_c B_c^{*+}$ of the hadronic molecule \mathfrak{M} . We calculate the strong couplings g_1 and g_2 at the vertices $\mathfrak{M} J/\psi B_c^+$ and $\mathfrak{M} \eta_c B_c^{*+}$, respectively: They are necessary to find the partial widths of these processes. To this end, we invoke technical tools of the three-point SR method and evaluate the form factors $g_1(q^2)$ and $g_2(q^2)$. At the mass shells of the mesons J/ψ and η_c the form factors $g_1(m_{J/\psi}^2)$ and $g_2(\eta_c^2)$ give the required strong couplings g_1 and g_2 .

A. $\mathfrak{M} \rightarrow J/\psi B_c^+$

The three-point correlation function to extract the sum rule for the form factor $g_1(q^2)$ is given by the expression

$$\Pi_{\mu\nu}^1(p, p') = i^2 \int d^4x d^4y e^{ip'y} e^{-ipx} \langle 0 | \mathcal{T} \{ I^{B_c}(y) I_\mu^{J/\psi}(0) I_\nu^\dagger(x) \} | 0 \rangle, \quad (14)$$

where $I^{B_c}(x)$ and $I_\mu^{J/\psi}$ are currents that correspond to mesons B_c^+ and J/ψ , respectively. They are introduced by the formulas

$$I_\mu^{J/\psi}(x) = \bar{c}_i(x) \gamma_\mu c_i(x), \quad I^{B_c}(x) = \bar{b}_j(x) i \gamma_5 c_j(x). \quad (15)$$

The correlator $\Pi_{\mu\nu}^1(p, p')$ written down using masses and decay constants (current coupling) of the particles \mathfrak{M} , J/ψ , and B_c^+ forms the phenomenological side $\Pi_{\mu\nu}^{1\text{Phys}}(p, p')$ of SR. After dissecting the contribution of the ground-state particles in the factorization approximation [36–38], it has the form

$$\begin{aligned} \Pi_{\mu\nu}^{1\text{Phys}}(p, p') &= \frac{\langle 0 | I^{B_c} | B_c^+(p') \rangle \langle 0 | I_\mu^{J/\psi} | J/\psi(q, \varepsilon) \rangle \langle J/\psi(q, \varepsilon) B_c^+(p') | \mathfrak{M}(p, \epsilon) \rangle}{p'^2 - m_{B_c}^2} \frac{1}{q^2 - m_{J/\psi}^2} \\ &\times \frac{\langle \mathfrak{M}(p, \epsilon) | I_\nu^\dagger | 0 \rangle}{p^2 - m^2} + \dots, \end{aligned} \quad (16)$$

where $m_{B_c} = (6274.47 \pm 0.27 \pm 0.17) \text{ MeV}$ and $m_{J/\psi} = (3096.900 \pm 0.006) \text{ MeV}$ are the masses of the mesons B_c^+ and J/ψ [35], while ε_μ is the polarization vector of the charmonium J/ψ .

After applying the matrix elements of the mesons B_c^+ and J/ψ

$$\langle 0 | I_\mu^{J/\psi} | J/\psi(q, \varepsilon) \rangle = f_{J/\psi} m_{J/\psi} \varepsilon_\mu, \quad \langle 0 | I^{B_c} | B_c^+(p') \rangle = \frac{f_{B_c} m_{B_c}^2}{m_b + m_c}, \quad (17)$$

as well as the matrix element for the vertex

$$\langle J/\psi(q, \varepsilon) B_c^+(p') | \mathfrak{M}(p, \epsilon) \rangle = g_1(q^2) [(\epsilon \cdot p')(\epsilon \cdot \varepsilon^*) - (p' \cdot \epsilon)(p \cdot \varepsilon^*)]. \quad (18)$$

we can express $\Pi_{\mu\nu}^{1\text{Phys}}(p, p')$ using the physical parameters of \mathfrak{M} , J/ψ , and B_c^+ involved into decay process. As a result, we find

$$\begin{aligned} \Pi_{\mu\nu}^{1\text{Phys}}(p, p') &= \frac{g_1(q^2) \Lambda f_{B_c} m_{B_c}^2 f_{J/\psi} m_{J/\psi}}{(m_b + m_c) (p^2 - m^2) (p'^2 - m_{B_c}^2) (q^2 - m_{J/\psi}^2)} \frac{1}{(q^2 - m_{J/\psi}^2)} \left[\frac{m^2 + m_{B_c}^2 - q^2}{2} g_{\mu\nu} \right. \\ &\left. - \frac{m^2}{m_{J/\psi}^2} p'_\mu p'_\nu + \frac{m^2 - m_{J/\psi}^2}{m_{J/\psi}^2} p'_\mu p_\nu - \frac{m^2 + m_{B_c}^2 - q^2}{2m_{J/\psi}^2} (p_\mu p_\nu + p_\mu p'_\nu) \right] + \dots \end{aligned} \quad (19)$$

In Eqs. (17) and (19) $f_{J/\psi} = (411 \pm 7)$ MeV and $f_{B_c} = (371 \pm 37)$ MeV are the decay constants of J/ψ and B_c^+ [39, 40], respectively.

The QCD side of SR is determined by the correlator $\Pi_{\mu\nu}^{1\text{OPE}}(p, p')$

$$\begin{aligned} \Pi_{\mu\nu}^{1\text{OPE}}(p, p') = & - \int d^4x d^4y e^{ip'y} e^{-ipx} \{ \text{Tr} [\gamma_\mu S_c^{ja}(-x) \gamma_\nu S_c^{aj}(x)] \text{Tr} [\gamma_5 S_c^{ib}(y-x) \gamma_5 S_b^{bi}(x-y)] \\ & - \text{Tr} [\gamma_5 S_c^{ia}(y-x) \gamma_\nu S_c^{aj}(x) \gamma_\mu S_c^{jb}(-x) \gamma_5 S_b^{bi}(x-y)] \}. \end{aligned} \quad (20)$$

The correlation functions $\Pi_{\mu\nu}^{1\text{Phys}}(p, p')$ and $\Pi_{\mu\nu}^{1\text{OPE}}(p, p')$ contains different Lorentz structures. We choose to work with the invariant amplitudes $\Pi_1^{\text{Phys}}(p^2, p'^2, q^2)$ and $\Pi_1^{\text{OPE}}(p^2, p'^2, q^2)$ which are related to terms $\sim g_{\mu\nu}$.

Having equated the functions $\Pi_1^{\text{Phys}}(p^2, p'^2, q^2)$ and $\Pi_1^{\text{OPE}}(p^2, p'^2, q^2)$, performed the double Borel transformations (over the variables $-p^2, -p'^2$), and subtracted contributions of suppressed terms, we get SR for $g_1(q^2)$

$$g_1(q^2) = \frac{2(m_b + m_c)}{\Lambda f_{B_c} m_{B_c}^2 f_{J/\psi} m_{J/\psi}} \frac{q^2 - m_{J/\psi}^2}{m^2 + m_{B_c}^2 - q^2} e^{m^2/M_1^2} e^{m_{B_c}^2/M_2^2} \Pi_1(\mathbf{M}^2, \mathbf{s}_0, q^2). \quad (21)$$

Here, $\Pi_1(\mathbf{M}^2, \mathbf{s}_0, q^2)$ is the amplitude $\Pi_1^{\text{OPE}}(p^2, p'^2, q^2)$ after the double Borel transformation and continuum subtractions. It is given by the formula

$$\Pi_1(\mathbf{M}^2, \mathbf{s}_0, q^2) = \int_{(3m_c+m_b)^2}^{s_0} ds \int_{(m_b+m_c)^2}^{s'_0} ds' \rho_1(s, s', q^2) e^{-s/M_1^2} e^{-s'/M_2^2}, \quad (22)$$

where spectral density $\rho(s, s', q^2)$ is determined as the imaginary part of $\Pi_1^{\text{OPE}}(s, s', q^2)$.

The function $\Pi_1(\mathbf{M}^2, \mathbf{s}_0, q^2)$ depends on two pairs of parameters (M_1^2, s_0) and (M_2^2, s'_0) . The first of them corresponds to the channel of the molecule \mathfrak{M} , while (M_2^2, s'_0) is related to the channel of B_c^+ meson. They are restricted in accord with standard rules of SR calculations. Our studies prove that Eq. (11) for the parameters (M_1^2, s_0) and

$$M_2^2 \in [6.5, 7.5] \text{ GeV}^2, \quad s'_0 \in [45, 47] \text{ GeV}^2. \quad (23)$$

meet SR restrictions.

It is known that the SR method leads to credible results in the Euclidean region $q^2 < 0$, whereas $g_1(q^2)$ amounts to g_1 at $q^2 = m_{J/\psi}^2$. Hence, it is convenient to make use of new function $g_1(Q^2)$ where $Q^2 = -q^2$, and employ it for subsequent investigations. The QCD results for $g_1(Q^2)$ where $Q^2 = 2 - 30 \text{ GeV}^2$ are plotted in Fig. 3.

To extract g_1 at $q^2 = -Q^2 = m_{J/\psi}^2$, we employ the extrapolating function $\mathcal{Z}_1(Q^2)$: At $Q^2 > 0$ it is equal to the SR data, but can be applied in the region of $Q^2 < 0$. We fix $\mathcal{Z}_1(Q^2)$ in the following form

$$\mathcal{Z}_i(Q^2) = \mathcal{Z}_i^0 \exp \left[z_i^1 \frac{Q^2}{m^2} + z_i^2 \left(\frac{Q^2}{m^2} \right)^2 \right], \quad (24)$$

where the parameters \mathcal{Z}_i^0 , z_i^1 , and z_i^2 are estimated from comparison of $\mathcal{Z}_1(Q^2)$ and SR data. It is not difficult to find that

$$\mathcal{Z}_1^0 = 0.945 \text{ GeV}^{-1}, \quad z_1^1 = 11.85, \quad z_1^2 = -8.66. \quad (25)$$

In Fig. 3 we plot also $\mathcal{Z}_1(Q^2)$, in which nice agreement of $\mathcal{Z}_1(Q^2)$ and SR data is evident. Then, for g_1 we get

$$g_1 \equiv \mathcal{Z}_1(-m_{J/\psi}^2) = (2.61 \pm 0.50) \times 10^{-1} \text{ GeV}^{-1}. \quad (26)$$

This result has been found by using Eq. (24). At the same time, SR data can be extended into region the region $Q^2 < 0$ by employing different extrapolating functions. To clarify this problem, we examine the fit function

$$\mathcal{Z}_{1A}(Q^2) = \frac{c_0}{(1 - Q^2/m^2)^4 [1 - c_1(Q^2/m^2) + c_2(Q^4/m^4)]}, \quad (27)$$

where c_0 , c_1 , and c_2 are fitted constants. We get $c_0 = 0.826 \text{ GeV}^{-1}$, $c_1 = 1.844$, and $c_2 = 2.731$ from comparison of Eq. (27) and SR data. This function is presented in Fig. 3 as well, in which one sees that it agrees with SR data and $\mathcal{Z}_1(Q^2)$. The fit function $\mathcal{Z}_{1A}(Q^2)$ leads to the result $g_1 = 0.158 \text{ GeV}^{-1}$, which deviates $|0.003|$ from the value in Eq. (26). But this deviation is more than an order of magnitude smaller than uncertainties ± 0.05 of g_1 arising from the

sum rule method. For this reason, we neglect uncertainties appearing due to the choice of extrapolating functions and employ Eq. (24) in our computations. It is worth noting that analytical forms of the extrapolating functions $\mathcal{Z}_1(Q^2)$ and $\mathcal{Z}_{1A}(Q^2)$ are inspired by the SR for $g_1(q^2)$ in Eq. (21), which contains both the exponential and $(m^2 - q^2)$ -type factors.

The width of the decay $\mathfrak{M} \rightarrow J/\psi B_c^+$ is computed using the formula

$$\Gamma [\mathfrak{M} \rightarrow J/\psi B_c^+] = g_1^2 \frac{\lambda_1}{24\pi m^2} |M_1|^2. \quad (28)$$

Here,

$$|M_1|^2 = \frac{1}{4m_{B_c}^2} \left[m^6 - 2m^4 m_{J/\psi}^2 + 2m_{B_c}^2 (m_{B_c}^2 - m_{J/\psi}^2)^2 + m^2 (m_{J/\psi}^4 + 6m_{J/\psi}^2 m_{B_c}^2 - 3m_{B_c}^4) \right]. \quad (29)$$

We have also employed $\lambda_1 = \lambda(m, m_{B_c}, m_{J/\psi})$ where $\lambda(a, b, c)$ is

$$\lambda(a, b, c) = \frac{\sqrt{a^4 + b^4 + c^4 - 2(a^2b^2 + a^2c^2 + b^2c^2)}}{2a}. \quad (30)$$

As a result, one finds

$$\Gamma [\mathfrak{M} \rightarrow J/\psi B_c^+] = (40.6 \pm 12.4) \text{ MeV}. \quad (31)$$

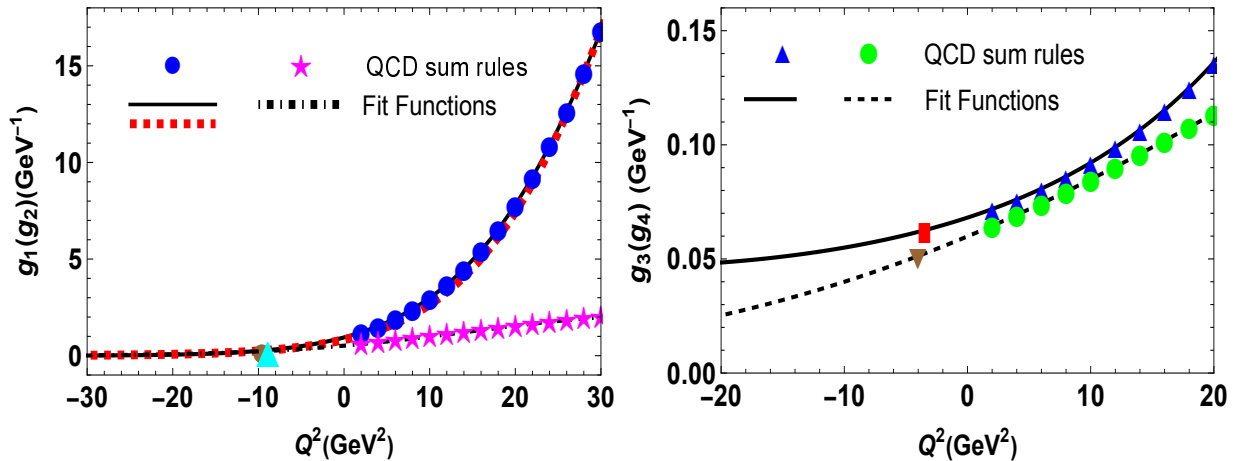


FIG. 3: Left panel: SR data and fit functions $\mathcal{Z}_1(Q^2)$ (solid curve), $\mathcal{Z}_{1A}(Q^2)$ (dashed line) and $\mathcal{Z}_2(Q^2)$ (dot-dashed line). The triangle and circle denote values of the extrapolating functions at the points $Q^2 = -m_{J/\psi}^2$ and $Q^2 = -m_{\eta_c}^2$, respectively. Right panel: QCD data and extrapolating functions $\mathcal{Z}_3(Q^2)$ (solid) and $\mathcal{Z}_4(Q^2)$ (dashed). The rectangle and triangle fix fit functions at the points $Q^2 = -m_{D^0}^2$ and $Q^2 = -m_{D^{*0}}^2$.

B. $\mathfrak{M} \rightarrow \eta_c B_c^{*+}$

To explore the channel $\mathfrak{M} \rightarrow \eta_c B_c^{*+}$ we estimate the coupling g_2 at the vertex $\mathfrak{M} \eta_c B_c^{*+}$. To this end, it is convenient to consider the correlation function $\Pi_{\mu\nu}^2(p, p')$

$$\Pi_{\mu\nu}^2(p, p') = i^2 \int d^4x d^4y e^{ip'y} e^{-ipx} \langle 0 | \mathcal{T} \{ I_\mu^{B_c^*}(y) I^\nu(0) I_\nu^\dagger(x) \} | 0 \rangle. \quad (32)$$

In Eq. (32) $I^\nu(x)$ and $I_\mu^{B_c^*}(x)$ are the interpolating currents for the mesons η_c and B_c^{*+}

$$I^\nu(x) = \bar{c}_i(x) i\gamma_5 c_i(x), \quad I_\mu^{B_c^*}(x) = \bar{b}_j(x) \gamma_\mu c_j(x). \quad (33)$$

The correlation function $\Pi_{\mu\nu}^{2\text{Phys}}(p, p')$ has the form

$$\Pi_{\mu\nu}^{2\text{Phys}}(p, p') = \frac{g_2(q^2)\Lambda f_{\eta_c} m_{\eta_c}^2 f_{B_c^*} m_{B_c^*}}{2m_c(p^2 - m^2)(p'^2 - m_{B_c^*}^2)(q^2 - m_{\eta_c}^2)} \left[\frac{m^2 - m_{B_c^*}^2 + q^2}{2} g_{\mu\nu} - p_\mu p_\nu + p'_\mu p'_\nu + \frac{m^2 + m_{B_c^*}^2 - q^2}{m_{B_c^*}^2} p_\mu p'_\nu \right] + \dots \quad (34)$$

To find $\Pi_{\mu\nu}^{2\text{Phys}}(p, p')$ the matrix elements

$$\langle 0 | I_{\mu_c}^{B_c^*} | B_c^{*+}(p', \varepsilon) \rangle = f_{B_c^*} m_{B_c^*} \varepsilon_\mu, \quad \langle 0 | I^{\eta_c} | \eta_c(q) \rangle = \frac{f_{\eta_c} m_{\eta_c}^2}{2m_c}, \quad (35)$$

and

$$\langle \eta_c(q) B_c^{*+}(p', \varepsilon) | \mathfrak{M}(p, \varepsilon) \rangle = g_2(q^2) [(p \cdot q)(\varepsilon \cdot \varepsilon^*) - (q \cdot \varepsilon)(p \cdot \varepsilon^*)], \quad (36)$$

have been used. Above, $m_{\eta_c} = (2984.1 \pm 0.4)$ MeV and $f_{\eta_c} = (421 \pm 35)$ MeV are parameters of the charmonium η_c . The mass $m_{B_c^*} = 6338$ MeV and $f_{B_c^*} = 471$ MeV are model predictions obtained in Refs. [41, 42].

The QCD side of the SR is given by the formula

$$\Pi_{\mu\nu}^{2\text{OPE}}(p, p') = \int d^4x d^4y e^{ip'y} e^{-ipx} \text{Tr} [\gamma_\mu S_c^{ia}(y-x) \gamma_\nu S_c^{aj}(x) \gamma_5 S_c^{jb}(-x) \gamma_5 S_b^{bi}(x-y)]. \quad (37)$$

To proceed we use the invariant amplitudes $\Pi_2^{\text{Phys}}(p^2, p'^2, q^2)$ and $\Pi_2^{\text{OPE}}(p^2, p'^2, q^2)$ related to structures $\sim g_{\mu\nu}$ both in the physical and OPE versions of the correlator $\Pi_{\mu\nu}^2(p, p')$. The SR for $g_2(q^2)$ derived after standard manipulations reads

$$g_2(q^2) = \frac{4m_c}{\Lambda f_{\eta_c} m_{\eta_c}^2 f_{B_c^*} m_{B_c^*}} \frac{q^2 - m_{\eta_c}^2}{m^2 - m_{B_c^*}^2 + q^2} e^{m^2/M_1^2} e^{m_{B_c^*}^2/M_2^2} \Pi_2(\mathbf{M}^2, \mathbf{s}_0, q^2), \quad (38)$$

respectively. The regions

$$M_2^2 \in [6.5, 7.5] \text{ GeV}^2, \quad s'_0 \in [49, 51] \text{ GeV}^2, \quad (39)$$

in B_c^{*+} meson's channel satisfy required constraints of SR analysis. The corresponding fit function $\mathcal{Z}_2(Q^2)$ has the parameters

$$\mathcal{Z}_2^0 = 0.518 \text{ GeV}^{-1}, \quad z_1^1 = 7.07, \quad z_2^2 = -8.93. \quad (40)$$

The SR data and the function $\mathcal{Z}_2(Q^2)$ are also shown in Fig. 3. For the strong coupling g_2 , we find

$$g_2 \equiv \mathcal{Z}_2(-m_{B_c^*}^2) = (2.5 \pm 0.4) \times 10^{-1} \text{ GeV}^{-1}. \quad (41)$$

The width of the channel $\mathfrak{M} \rightarrow \eta_c B_c^{*+}$ is

$$\Gamma [\mathfrak{M} \rightarrow \eta_c B_c^{*+}] = (36.8 \pm 9.5) \text{ MeV}. \quad (42)$$

IV. SUBDOMINANT DECAYS $\mathfrak{M} \rightarrow B^{*+} D^0$, $B^{*0} D^+$, $B^+ D^{*0}$, AND $B^0 D^{*+}$

Annihilation of $\bar{c}c$ quarks generates numerous subdominant decay channels of the molecule $J/\psi B_c^+$. Processes $\mathfrak{M} \rightarrow B^{*+} D^0$, $B^{*0} D^+$, $B^+ D^{*0}$, and $B^0 D^{*+}$ are such decay modes. Importance of this mechanism to explore decays of exotic states was emphasized in Refs. [31–33] and used to explore decays of numerous tetraquarks. It was also applied to investigate processes with hadronic molecules [22–24, 29]

It is worth emphasizing that some of these decays have parameters very close to each other. The reason is that in the limit $m_u = m_d = 0$, which is adopted in this work, phenomenological components of the relevant SRs for the decays $\mathfrak{M} \rightarrow B^{*+} D^0$ and $B^{*0} D^+$ differ by the masses and decay constants of, for instance, D^0 and D^+ mesons. The QCD components of the sum rules contain u and d quarks' propagators identical in this case. Because we ignore small differences in the masses and decay constants of the mesons, the SRs lead to the same predictions of their parameters. Hence, we treat these decays as identical processes and calculate the partial width of the channel $\mathfrak{M} \rightarrow B^{*+} D^0$: The width of the second mode is equal to that of the first one. These arguments are also valid for the pair of processes $\mathfrak{M} \rightarrow B^+ D^{*0}$ and $\mathfrak{M} \rightarrow B^0 D^{*+}$.

A. $\mathfrak{M} \rightarrow B^{*+} D^0$ and $B^{*0} D^+$

Here, we study the mode $\mathfrak{M} \rightarrow B^{*+} D^0$ and calculate its partial decay width. We plan to determine the strong coupling g_3 of particles at $\mathfrak{M} B^{*+} D^0$. The correlation function to be considered is

$$\Pi_{\mu\nu}^3(p, p') = i^2 \int d^4x d^4y e^{ip'y} e^{-ipx} \langle 0 | \mathcal{T} \{ I_\mu^{B^*}(y) I_\nu^{D^0}(0) I_\nu^\dagger(x) \} | 0 \rangle, \quad (43)$$

where $I_\mu^{B^*}$ and $I^{D^0}(x)$ are currents for the particles B^{*-} and D^0 mesons

$$I_\mu^{B^*}(x) = \bar{b}_i(x) \gamma_\mu u_i(x), \quad I^{D^0}(x) = \bar{u}_j(x) i \gamma_5 c_j(x). \quad (44)$$

The phenomenological formula for $\Pi_{\mu\nu}^3(p, p')$ is found by means of the expressions

$$\langle 0 | I_\mu^{B^*} | B^{*+}(p', \varepsilon) \rangle = f_{B^*} m_{B^*} \varepsilon_\mu, \quad \langle 0 | I^{D^0} | D^0(q) \rangle = \frac{f_D m_{D^0}^2}{m_c}. \quad (45)$$

The characteristics of the particles above are $m_{B^*} = (5324.75 \pm 0.20)$ MeV, $m_{D^0} = (1864.84 \pm 0.05)$ MeV and $f_{B^*} = (210 \pm 6)$ MeV, $f_D = (211.9 \pm 1.1)$ MeV. In Eq. (45) the polarization vector of the vector meson B^{*+} is denoted by ε_μ . The vertex $\langle B^{*+}(p', \varepsilon) D^0(q) | \mathfrak{M}(p, \epsilon) \rangle$ and $\Pi_{\mu\nu}^{3\text{Phys}}(p, p')$ are similar to expressions presented in the previous section III.

Computations of $\Pi_{\mu\nu}^3(p, p')$ yield

$$\Pi_{\mu\nu}^{3\text{OPE}}(p, p') = \frac{1}{3} \int d^4x d^4y e^{ip'y} e^{-ipx} \langle \bar{c}c \rangle \text{Tr} [\gamma_\mu S_u^{ij}(y) \gamma_5 S_c^{ja}(-x) \gamma_\nu \gamma_5 S_b^{ia}(x-y)]. \quad (46)$$

The correlation function $\Pi_{\mu\nu}^{3\text{OPE}}(p, p')$ depends on three quark propagators and vacuum condensate $\langle \bar{c}c \rangle$, and differs from standard correlators which contain four quark propagators. In our computations we contract heavy and light quark fields. The mesons $B^{*+} D^0$ contain only one c -quark field, as a result, free $\bar{c}c$ quarks in \mathfrak{M} form a local vacuum condensate. In other words, $\langle \bar{c}c \rangle$ appears in formulas instead of the quark propagator and is considering on equal footing with them.

In what follows, we apply the relation between the heavy quark and gluon condensates to express $\Pi_{\mu\nu}^{3\text{OPE}}(p, p')$ using relevant parameters. The available formula for $\langle \bar{c}c \rangle$ reads [25, 43, 44]

$$m_c \langle \bar{c}c \rangle = -\frac{1}{12} \langle \frac{\alpha_s G^2}{\pi} \rangle + \frac{1}{m_c^2} \langle \frac{\alpha_s G^3}{\pi} \rangle \left(-\frac{1}{48} + \frac{13}{720} \right) + \dots \quad (47)$$

In our analysis we use only the first term in Eq. (47) extracted in Ref. [25], because next ones are suppressed by additional powers of m_c^{-1} and are small.

The form factor $g_3(Q^2)$ is evaluated in the domain $Q^2 = 2 - 20$ GeV²: At $Q^2 = -m_{D^0}^2$ it equals to g_3 . For (M_1^2, s_0) we have used Eq. (11), and (M_2^2, s'_0) have changed in the regions

$$M_2^2 \in [5.5, 6.5] \text{ GeV}^2, \quad s'_0 \in [34, 35] \text{ GeV}^2. \quad (48)$$

Results for $g_3(Q^2)$ are depicted in Fig. 3. The fit function $\mathcal{Z}_3(Q^2)$ is fixed by the parameters $\mathcal{Z}_3^0 = 0.068$ GeV⁻¹, $z_3^1 = 2.46$, and $z_3^2 = 3.95$. The coupling g_3 is found at $q^2 = -Q^2 = m_{D^0}^2$ and amounts to

$$g_3 \equiv \mathcal{Z}_3(-m_{D^0}^2) = (6.3 \pm 1.2) \times 10^{-2} \text{ GeV}^{-1}. \quad (49)$$

For the width of the process $\mathfrak{M} \rightarrow B^{*+} D^0$ our analysis predicts

$$\Gamma [\mathfrak{M} \rightarrow B^{*+} D^0] = (9.7 \pm 3.0) \text{ MeV}. \quad (50)$$

Note that ambiguities above are due to ones in g_3 and in the masses of the molecule \mathfrak{M} , and mesons B^{*+} and D^0 .

The width of the next decay $\mathfrak{M} \rightarrow B^{*0} D^+$ is estimated using the formula

$$\Gamma [\mathfrak{M} \rightarrow B^{*0} D^+] \approx \Gamma [\mathfrak{M} \rightarrow B^{*+} D^0]. \quad (51)$$

B. $\mathfrak{M} \rightarrow B^+ D^{*0}$ and $B^0 D^{*+}$

The pair of the decay modes $\mathfrak{M} \rightarrow B^+ D^{*0}$ and $\mathfrak{M} \rightarrow B^0 D^{*+}$ is explored in this subsection using the same techniques. Below, we give parameters of the process $\mathfrak{M} \rightarrow B^+ D^{*0}$ bearing in mind that the second mode approximately shares those of the first channel.

We consider the correlation function

$$\Pi_{\mu\nu}^4(p, p') = i^2 \int d^4x d^4y e^{ip'y} e^{-ipx} \langle 0 | \mathcal{T} \{ I^{B^+}(y) I_\mu^{D^{*0}}(0) I_\nu^\dagger(x) \} | 0 \rangle. \quad (52)$$

Here, $I^{B^+}(x)$ and $I_\mu^{D^{*0}}(x)$ are currents which correspond to mesons B^+ and D^{*0} , respectively

$$I^{B^+}(x) = \bar{b}_i(x) i \gamma_5 u_i(x), \quad I_\mu^{D^{*0}}(x) = \bar{u}_j(x) \gamma_\mu c_j(x). \quad (53)$$

The correlation function Eq. (52) is necessary to determine the SR for the form factor $g_4(q^2)$. At the mass shell of the meson D^{*0} this form factor allows one to get the strong coupling g_4 at the vertex $\mathfrak{M} B^+ D^{*0}$.

We evaluate the function $\Pi_{\mu\nu}^{4\text{Phys}}(p, p')$ using the matrix elements

$$\langle 0 | I^{B^+} | B^-(p') \rangle = \frac{f_B m_B^2}{m_b}, \quad \langle 0 | I_\mu^{D^{*0}} | D^{*0}(q, \varepsilon) \rangle = f_{D^{*0}} m_{D^{*0}} \varepsilon_\mu, \quad (54)$$

where $m_B = (5279.41 \pm 0.07)$ MeV, $f_B = 206$ MeV and $m_{D^{*0}} = (2006.85 \pm 0.05)$ MeV, $f_{D^{*0}} = (252.2 \pm 22.66)$ MeV are parameters of the particles under discussion. By ε_μ we denote the polarization vector of the D^{*0} meson. The vertex element $\langle B^+(p') D^{*0}(q, \varepsilon) | \mathfrak{M}(p, \epsilon) \rangle$ is introduced in the following form

$$\langle B^+(p') D^{*0}(q, \varepsilon) | \mathfrak{M}(p, \epsilon) \rangle = g_4(q^2) [(p \cdot p')(\epsilon \cdot \varepsilon^*) - (p' \cdot \epsilon)(p \cdot \varepsilon^*)]. \quad (55)$$

The QCD side of SR is given by the expression

$$\Pi_{\mu\nu}^{4\text{OPE}}(p, p') = \frac{1}{3} \int d^4x d^4y e^{ip'y} e^{-ipx} \langle \bar{c}c \rangle \text{Tr} [\gamma_5 S_u^{ij}(y) \gamma_\mu S_c^{ja}(-x) \gamma_\nu \gamma_5 S_b^{ai}(x-y)]. \quad (56)$$

Numerical computations of $g_4(Q^2)$ is performed at $Q^2 = 2 - 20$ GeV² using the regions Eq. (11) for (M_1^2, s_0) and

$$M_2^2 \in [5.5, 6.5] \text{ GeV}^2, \quad s'_0 \in [33.5, 34.5] \text{ GeV}^2, \quad (57)$$

for the Borel and continuum subtraction parameters (M_2^2, s'_0) . The extrapolating function $\mathcal{Z}_4(Q^2)$ that has been employed to compute the coupling $g_4(Q^2)$ is fixed by the following constants $\mathcal{Z}_4^0 = 0.060$ GeV⁻¹, $z_4^1 = 3.57$, $z_4^2 = -2.50$ and shown also in Fig. 3. This function leads to the predictions

$$g_4 \equiv \mathcal{Z}_4(-m_{D^{*0}}^2) = (5.1 \pm 0.9) \times 10^{-2} \text{ GeV}^{-1}, \quad (58)$$

and

$$\Gamma[\mathfrak{M} \rightarrow B^+ D^{*0}] = (6.6 \pm 1.7) \text{ MeV}. \quad (59)$$

The width of the channel $\mathfrak{M} \rightarrow B^0 D^{*+}$ is also equal to Eq. (59).

V. DECAYS TO STRANGE MESONS

Decays to strange mesons $\mathfrak{M} \rightarrow B_s^{*0} D_s^+$ and $B_s^0 D_s^{*+}$ are last two channels of \mathfrak{M} which have been studied in this article. To consider the decay $\mathfrak{M} \rightarrow B_s^{*0} D_s^+$ one should analyze the correlation function

$$\hat{\Pi}_{\mu\nu}^1(p, p') = i^2 \int d^4x d^4y e^{ip'y} e^{-ipx} \langle 0 | \mathcal{T} \{ I_\mu^{B_s^{*0}}(y) I_\nu^{D_s^+}(0) I_\nu^\dagger(x) \} | 0 \rangle, \quad (60)$$

which permits one to extract SR for the form factor $G_1(Q^2)$. In Eq. (60) $I_\mu^{B_s^{*0}}(x)$ and $I_\nu^{D_s^+}(x)$ are interpolating currents for the mesons B_s^{*0} and D_s^+

$$I_\mu^{B_s^{*0}}(x) = \bar{b}_i(x) \gamma_\mu s_i(x), \quad I_\nu^{D_s^+}(x) = \bar{s}_j(x) i \gamma_5 c_j(x). \quad (61)$$

To determine the physical component $\widehat{\Pi}_{\mu\nu}^{\text{Phys}}(p, p')$ of SR, we apply the matrix elements

$$\langle 0 | I_{\mu}^{B^*} | B_s^{*0}(p', \epsilon) \rangle = f_{B_s^*} m_{B_s^*} \epsilon_{\mu}, \quad \langle 0 | I^{D_s} | D_s^+(q) \rangle = \frac{f_{D_s} m_{D_s}^2}{m_c + m_s}. \quad (62)$$

In Eq. (62) $m_{B_s^*} = (5415.4 \pm 1.4)$ MeV, $f_{B_s^*} = 221$ MeV and $m_{D_s} = (1968.35 \pm 0.07)$ MeV, $f_{D_s} = (249.9 \pm 0.5)$ MeV are the parameters of the final-state mesons, and $m_s = (93.5 \pm 0.8)$ MeV is the mass of s -quark. The vertex $\langle B_s^{*0}(p', \epsilon) D_s^-(q) | \mathfrak{M}(p, \epsilon) \rangle$ has the standard form.

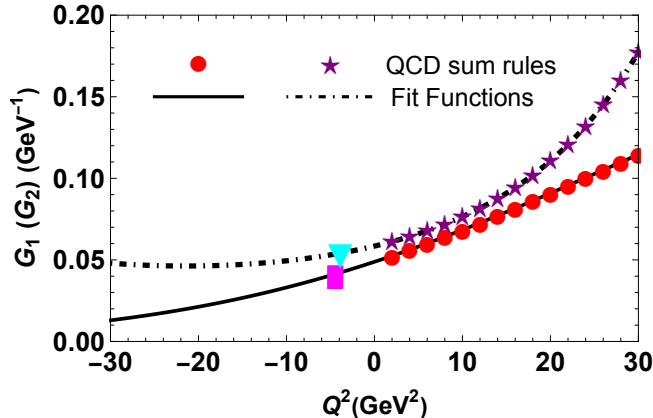


FIG. 4: SR data for $G_1(Q^2)$ and $G_2(Q^2)$, and extrapolating functions $\widehat{Z}_1(Q^2)$ (solid curve), and $\widehat{Z}_2(Q^2)$ (dot-dashed curve). Values of these functions at the points $Q^2 = -m_{D_s}^2$ and $Q^2 = -m_{D_s}^2$ are shown by the rectangle and triangle, respectively.

Computation of the correlator $\widehat{\Pi}_{\mu\nu}^1(p, p')$ in terms of the heavy quark propagators yields

$$\widehat{\Pi}_{\mu\nu}^{\text{OPE}}(p, p') = \frac{1}{3} \int d^4x d^4y e^{ip'y} e^{-ipx} \langle \bar{c}c \rangle \text{Tr} [\gamma_{\mu} S_s^{ij}(y) \gamma_5 S_c^{ja}(-x) \gamma_{\nu} \gamma_5 S_b^{ai}(x-y)]. \quad (63)$$

The SR for the form factor $G_1(Q^2)$ is found by employing amplitudes in $\widehat{\Pi}_{\mu\nu}^{\text{Phys}}(p, p')$ and $\widehat{\Pi}_{\mu\nu}^{\text{OPE}}(p, p')$ corresponding to terms $\sim g_{\mu\nu}$.

Calculations are carried out using parameters

$$M_2^2 \in [6, 7] \text{ GeV}^2, \quad s'_0 \in [35, 36] \text{ GeV}^2, \quad (64)$$

for B_s^{*0} channel. The constants in the fit function $\widehat{Z}_1(Q^2)$ are $\widehat{Z}_1^0 = 0.0585 \text{ GeV}^{-1}$, $\widehat{Z}_1^1 = 2.068$, and $\widehat{Z}_1^2 = 4.569$. Results of numerical computations are plotted in Fig. 4, in which one can see the SR data for $Q^2 = 2 - 30 \text{ GeV}^2$, as well as the fit function $\widehat{Z}_1(Q^2)$.

Then the strong coupling G_1 is equal to

$$G_1 = \widehat{Z}_1(-m_{D_s}) = (5.4 \pm 1.0) \times 10^{-2} \text{ GeV}^{-1}. \quad (65)$$

The partial width of the decay $\mathfrak{M} \rightarrow B_s^{*0} D_s^+$ amounts to

$$\Gamma [\mathfrak{M} \rightarrow B_s^{*0} D_s^+] = (6.8 \pm 1.8) \text{ MeV}. \quad (66)$$

The channel $\mathfrak{M} \rightarrow B_s^0 D_s^{*+}$ is the next mode with the strange mesons in the final-state. It is also explored in accordance with the scheme applied till now. Thus, the correlator necessary for our analysis is

$$\widehat{\Pi}_{\mu\nu}^2(p, p') = i^2 \int d^4x d^4y e^{ip'y} e^{-ipx} \langle 0 | \mathcal{T} \{ I_{\mu}^{B_s}(y) I_{\nu}^{D_s^*}(0) I_{\nu}^{\dagger}(x) \} | 0 \rangle, \quad (67)$$

where

$$I^{B_s}(x) = \bar{b}_i(x) i \gamma_5 s_i(x), \quad I_{\mu}^{D_s^*}(x) = \bar{s}_j(x) \gamma_{\mu} c_j(x), \quad (68)$$

are the interpolating currents for mesons B_s^0 and D_s^{*+} , respectively. The physical side of the sum rule for the form factor $G_2(q^2)$ is determined by the expression

$$\begin{aligned} \widehat{\Pi}_{\mu\nu}^{2\text{Phys}}(p, p') = & \frac{G_2(q^2)\Lambda f_{B_s} m_{B_s}^2 f_{D_s^*} m_{D_s^*}}{(m_b + m_s)(p^2 - m^2)(p'^2 - m_{B_s}^2)(q^2 - m_{D_s^*}^2)} \frac{1}{(q^2 - m_{D_s^*}^2)} \left[\frac{m^2 + m_{B_s}^2 - q^2}{2} g_{\mu\nu} - \frac{m^2}{m_{D_s^*}^2} p'_\mu p'_\nu \right. \\ & \left. + \frac{m^2 - m_{D_s^*}^2}{m_{D_s^*}^2} p'_\mu p_\nu - \frac{m^2 + m_{B_s}^2 - q^2}{2m_{D_s^*}^2} (p_\mu p_\nu + p'_\mu p'_\nu) \right] + \dots \end{aligned} \quad (69)$$

This correlation function has been derived using the matrix elements

$$\langle 0 | I^{B_s} | B_s^{*0}(p') \rangle = \frac{f_{B_s} m_{B_s}^2}{m_b + m_s}, \quad \langle 0 | I_{\mu}^{D_s^*} | D_s^{*+}(q, \epsilon) \rangle = f_{D_s^*} m_{D_s^*} \epsilon_\mu, \quad (70)$$

and

$$\langle B_s^0(p') D_s^{*+}(q, \epsilon) | \mathfrak{M}(p, \epsilon) \rangle = G_2(q^2) [(p \cdot p')(\epsilon \cdot \epsilon^*) - (p' \cdot \epsilon)(p \cdot \epsilon^*)]. \quad (71)$$

In Eq. (70) $m_{B_s} = (5366.93 \pm 0.10)$ MeV, $m_{D_s^*} = (2112.2 \pm 0.4)$ MeV, and $f_{B_s} = 234$ MeV, $f_{D_s^*} = (268.8 \pm 6.5)$ MeV are the masses and decay constants of the final-state particles.

The QCD side $\widehat{\Pi}_{\mu\nu}^{2\text{OPE}}(p, p')$ is given by the formula

$$\widehat{\Pi}_{\mu\nu}^{2\text{OPE}}(p, p') = \frac{1}{3} \int d^4x d^4y e^{ip'y} e^{-ipx} \langle \bar{c}c \rangle \text{Tr} [\gamma_5 S_s^{ij}(y) \gamma_\mu S_c^{ja}(-x) \gamma_\nu \gamma_5 S_b^{ai}(x-y)]. \quad (72)$$

Numerical calculations are carried out using the parameters

$$M_2^2 \in [5.5, 6.5] \text{ GeV}^2, \quad s'_0 \in [34, 35] \text{ GeV}^2, \quad (73)$$

in the B_s^0 channel. The parameters of the fit function $\widehat{\mathcal{Z}}_2(Q^2)$ are $\widehat{\mathcal{Z}}_2^0 = 0.0488 \text{ GeV}^{-1}$, $\widehat{\mathcal{Z}}_2^1 = 3.495$, and $\widehat{\mathcal{Z}}_2^2 = -2.438$. The prediction for G_2 reads

$$G_2 = \widehat{\mathcal{Z}}_2(-m_{D_s^*}) = (4.1 \pm 0.8) \times 10^{-2} \text{ GeV}^{-1}. \quad (74)$$

Then, the partial width of the process $\mathfrak{M} \rightarrow B_s^0 D_s^{*+}$ is

$$\Gamma [\mathfrak{M} \rightarrow B_s^0 D_s^{*+}] = (3.9 \pm 1.1) \text{ MeV}. \quad (75)$$

Having utilized results obtained in this work, we estimate the full width of the molecule \mathfrak{M}

$$\Gamma [\mathfrak{M}] = (121 \pm 17) \text{ MeV}, \quad (76)$$

which characterizes it as a broad exotic state. Note that subdominant modes with the total width 43 MeV form approximately 36% of the parameter $\Gamma [\mathfrak{M}]$.

VI. DISCUSSION AND CONCLUDING REMARKS

Parameters of the structure(s) $J/\psi B_c^+$ [and $\eta_c B_c^{*+}$] shed light on its properties allowing one to draw some quantitative and qualitative conclusions about exotic heavy molecular states. The molecules $J/\psi B_c^+$ and $\eta_c B_c^{*+}$ are relatively new members of the hadron spectroscopy: There are only few works devoted to theoretical analysis of these systems. Because they have not been yet observed experimentally, the masses and widths of these structures evaluated in the present work are important for placing them in due positions inside of this family.

The mass $m = (9740 \pm 70)$ MeV has been extracted using the SR method with a rather high accuracy which means that the mass of the hadronic molecule is inside of the region $m \in [9660, 9810]$ MeV. This result permits us to conclude that $J/\psi B_c^+$ and $\eta_c B_c^{*+}$ lie above corresponding two-meson thresholds and easily breaks down to constituent mesons, because even in its lower value the mass $m = 9660$ MeV is considerably above the 9372 MeV threshold. In other words, the molecules $J/\psi B_c^+$ and $\eta_c B_c^{*+}$ are resonant structures and do not form bound states. Nevertheless,

we treat $J/\psi B_c^+$ and $\eta_c B_c^{*+}$ as highly unstable hadronic molecules because they are formed by two heavy mesons and their interpolating currents are constructed in accordance with these structures.

It is instructive to compare this situation with the axial-vector molecule(s) $\mathcal{M}_{AV} = \Upsilon B_c^-$ [and $\eta_b B_c^{*-}$] built of $bb\bar{b}\bar{c}$ quarks. It was demonstrated that the mass of \mathcal{M}_{AV} resides in the region [15710, 15890] MeV, and in the lower border of this interval 15710 MeV it is stable against decays to mesons ΥB_c^- and $\eta_b B_c^{*-}$. The reason is that this mass is smaller than corresponding kinematical thresholds 15735 MeV and 15737 MeV [30]. In this sense the mesons Υ and B_c^- , as well as η_b and B_c^{*-} may form bound-state axial-vector molecules. But even in this case they transform to ordinary mesons due to $\bar{b}b$ annihilations in these structures.

In other words, the axial-vector state ΥB_c^- is more stable against strong decays (in lower mass limit) than the molecule $J/\psi B_c^+$. A conclusion about stable nature of some of four-quark mesons containing bb quarks is not new for the tetraquark spectroscopy. Thus, it was found that axial-vector diquark-antidiquark state $T_{bb}^- = bb\bar{u}\bar{d}$ lies below the $B^-\bar{B}^{*0}$ and $B^-\bar{B}^0\gamma$ thresholds and is stable against the strong and radiative transformations [45–47]. Hence, it decays to conventional mesons via weak processes considered in Ref. [47]. The charmed counterpart of T_{bb}^- , i.e., a diquark-antidiquark state $T_{cc}^+ = cc\bar{u}\bar{d}$ is above a D^*D threshold and is not a stable particle [48]. It is remarkable that T_{cc}^+ was observed by the LHCb collaboration in $D^0D^0\pi^+$ mass distribution as a narrow peak with the width $\Gamma = (48 \pm 2_{-14}^{+0})$ keV [49, 50]. The mass of T_{cc}^+ is very close to the D^0D^{*+} threshold 3875.1 MeV, but is smaller than this limit. This discovery confirmed experimentally that the axial-vector state T_{cc}^+ is strong-interaction unstable structure. The resonance T_{cc}^+ were investigated in the context of diquark and hadronic molecule models in numerous publications (for details see, Refs. [51–54] and references therein).

In general, the two-meson continuum below m may affect predictions of sum rule computations, because the interpolating current $I_\mu(x)$ interacts with both the molecule \mathfrak{M} and this continuum. Contributions related to these interactions can be included into analysis by re-scaling the current coupling Λ and keeping m fixed [52]. But their numerical effects are small being around 2–3% of uncertainties in Λ while SR method generates approximately 10% ambiguities. Therefore, the prediction for m is stable against two-meson contamination.

The full width of $J/\psi B_c^+$ has been found by considering its different decay channels. We have computed the partial widths of the dominant decay modes $\mathfrak{M} \rightarrow J/\psi B_c^+$ and $\mathfrak{M} \rightarrow \eta_c B_c^{*+}$. The subdominant processes, which imply transformation of \mathfrak{M} to $B^{*+}D^0$, $B^{*0}D^+$, B^+D^{*0} , B^0D^{*+} , $B_s^{*0}D_s^+$ and $B_s^0D_s^{*+}$ mesons, have been explored as well. The dominant decay channels constitute 64% of $\Gamma[\mathfrak{M}]$, whereas subdominant modes form remaining 36%. Contributions of subdominant processes may be further refined by taking into account other possible channels. Our analysis demonstrates that the axial-vector molecule $J/\psi B_c^+$ with the full width (121 ± 17) MeV is the broad resonance above the relevant continuum.

Information on the partial widths of different decay channels as well as full width of the molecule \mathfrak{M} are important for experimental analysis of these particles. A broad peak in the mass distributions of final-state $J/\psi B_c^+$ or $\eta_c B_c^{*+}$ mesons in some processes would indicate on observation of all-heavy axial-vector exotic meson with quark content $cc\bar{c}\bar{b}$. But a diquark-antidiquark state $cc\bar{c}\bar{b}$ also decays through these channels. Therefore, a conclusion about internal structure of such a peak can only be made by comparing experimental results with theoretical predictions for widths of the molecule and diquark-antidiquark states. Similarly, some enhancements may be seen in the mass distributions, for instance, $B^{*+}D^0$ and $B^{*0}D^+$ mesons. But to interpret them as product of subdominant processes, one first needs to compute parameters of hadronic molecules $B^{*+}D^0$ and $B^{*0}D^+$ which may dissociate to these mesons as well. Because exotic hadronic molecules with asymmetric contents are new objects of studies these problems, in particular decays of such states, are waiting for their analyses.

Hadronic molecules built of only heavy quarks were on focus of studies in Ref. [16]. The authors used the extended local gauge formalism to explore such molecules. They did not find axial-vector bound states in $cc\bar{c}\bar{b}$ sector, which agree with our conclusions. But they did not give information on a mass(es) of possible resonant structures. In the lack of such calculations, it is interesting to compare our results with predictions made for relevant diquark-antidiquark states.

The diquark-antidiquark exotic mesons with different spin-parities and nonsymmetrical quark contents were studied in Refs. [55–61]. In these articles the authors used different methods and approaches such as nonrelativistic constituent quark, multi-quark color flux-tube, and chromomagnetic models, the Bethe-Salpeter equations and effective potential model to investigate fully heavy diquark-antidiquark structures. Consider, for instance last two publications. The constituent quark model was used to evaluate parameters of the fully heavy tetraquarks in Ref. [60], whereas the relativistic quark model employed in the second paper [61]. The mass of the axial-vector tetraquark $cc\bar{c}\bar{b}$ in these articles were found equal to 9706 MeV and 9611 MeV, respectively. First, one sees a 100 MeV discrepancy in predictions of different methods. Nevertheless, we fix the mass gaps around of 34 MeV and 130 MeV between diquark-antidiquark and molecular states of the same content, which are natural for particles with different internal organizations: Colored diquarks and antidiquarks form more tightly bound compounds than ordinary colorless mesons.

The molecules $J/\psi B_c^+$ and $\eta_c B_c^{*+}$ are only building units of the physical states with asymmetric quark content.

Real particles may be formed owing to mixing of the molecules \mathfrak{M} and $\widetilde{\mathfrak{M}}$. Transitions between molecules $J/\psi B_c^+$ and $\eta_c B_c^{*+}$ as well as their mixing with axial-vector tetraquark $cc\bar{c}\bar{b}$ are among possible scenarios. But related problems require additional detailed studies which are beyond of the current article.

In the present work we have calculated the mass and width of the resonant state(s) $J/\psi B_c^+$ [and $\eta_c B_c^{*+}$]. These results are important to understand the inner structures and properties of the axial-vector molecules $J/\psi B_c^+$ and $\eta_c B_c^{*+}$. The current analysis has clarified only small piece of the whole picture called "fully heavy exotic mesons". But a lot of efforts should be made to see it in all details: Comparison of our predictions and alternative ones fills out blanks in our knowledge about features of these states.

-
- [1] M. Bander, G. L. Shaw, P. Thomas, and S. Meshkov, Phys. Rev. Lett. **36**, 695 (1976).
[2] M. B. Voloshin and L. B. Okun, JETP Lett. **23**, 333 (1976).
[3] A. De Rujula, H. Georgi, and S. L. Glashow, Phys. Rev. Lett. **38**, 317 (1977).
[4] R. Molina and E. Oset, Phys. Lett. D **811**, 135878 (2020) [Erratum: Phys. Lett. D **837**, 137645 (2023)].
[5] Y. J. Xu, Y. L. Liu, C. Y. Cui, and M. Q. Huang, Phys. Rev. D **104**, 094028 (2021).
[6] Q. Xin and Z. G. Wang, Eur. Phys. J. A **58**, 110 (2022).
[7] F. L. Wang, S. Q. Luo, and X. Liu, Phys. Rev. D **107**, 114017 (2023).
[8] S. S. Agaev, K. Azizi, and H. Sundu, J. Phys. G **50**, 055002 (2023).
[9] S. S. Agaev, K. Azizi, and H. Sundu, Phys. Rev. D **107**, 094019 (2023).
[10] E. Braaten, L. P. He, K. Ingles, and J. Jiang, JHEP **02**, 163 (2024).
[11] Q. Wu, M. Z. Liu and L. S. Geng, Eur. Phys. J. C **84**, 147 (2024).
[12] W. H. Liang, T. Ban, and E. Oset, Phys. Rev. D **109**, 054030 (2024).
[13] F. Wang, G. Li, S. D. Liu, and Q. Wu, Phys. Rev. D **111**, 094001 (2025).
[14] N. Yalikun, X. K. Dong, and U. G. Meißner, Phys. Rev. D **111**, 094036 (2025).
[15] W. Y. Liu and H. X. Chen, Eur. Phys. J. C **85**, 636 (2025).
[16] W. Y. Liu and H. X. Chen, Universe **11**, 36 (2025).
[17] R. Aaij *et al.* (LHCb Collaboration), Sci. Bull. **65**, 1983 (2020).
[18] G. Aad *et al.* (ATLAS Collaboration), Phys. Rev. Lett. **131**, 151902 (2023).
[19] A. Hayrapetyan *et al.* (CMS Collaboration), Phys. Rev. Lett. **132**, 111901 (2024).
[20] S. S. Agaev, K. Azizi, B. Barsbay and H. Sundu, Eur. Phys. J. Plus **138**, 935 (2023).
[21] S. S. Agaev, K. Azizi, B. Barsbay and H. Sundu, Eur. Phys. J. C **83**, 994 (2023).
[22] S. S. Agaev, K. Azizi, and H. Sundu, Phys. Rev. D **112**, 054001 (2025).
[23] S. S. Agaev, K. Azizi, and H. Sundu, Phys. Lett. B **870**, 139885 (2025).
[24] S. S. Agaev, K. Azizi, and H. Sundu, Phys. Lett. B **871**, 140014 (2025).
[25] M. A. Shifman, A. I. Vainshtein and V. I. Zakharov, Nucl. Phys. B **147**, 385 (1979).
[26] M. A. Shifman, A. I. Vainshtein and V. I. Zakharov, Nucl. Phys. B **147**, 448 (1979).
[27] R. M. Albuquerque, J. M. Dias, K. P. Khemchandani, A. Martinez Torres, F. S. Navarra, M. Nielsen and C. M. Zanetti, J. Phys. G **46**, 093002 (2019).
[28] S. S. Agaev, K. Azizi and H. Sundu, Turk. J. Phys. **44**, 95 (2020).
[29] S. S. Agaev, K. Azizi, and H. Sundu, Eur. Phys. J. A, to be published, arXiv:2511.03541 [hep-ph].
[30] S. S. Agaev, K. Azizi, and H. Sundu, Eur. Phys. J. A **62**, 59 (2026).
[31] C. Becchi, A. Giachino, L. Maiani, and E. Santopinto, Phys. Lett. B **806**, 135495 (2020).
[32] C. Becchi, A. Giachino, L. Maiani, and E. Santopinto, Phys. Lett. B **811**, 135952 (2020).
[33] S. S. Agaev, K. Azizi, B. Barsbay, and H. Sundu, Phys. Rev. D **109**, 014006 (2024).
[34] S. S. Agaev, K. Azizi, B. Barsbay, and H. Sundu, Eur. Phys. J. A **61**, 118 (2025).
[35] S. Navas *et al.* [Particle Data Group], Phys. Rev. D **110**, 030001 (2024).
[36] B. L. Ioffe, and A. V. Smilga, Nucl. Phys. B **216**, 373 (1983).
[37] P. Colangelo, and A. Khodjamirian, hep-ph/0010175.
[38] S. S. Agaev, K. Azizi and H. Sundu, Phys. Rev. D **106**, 014025 (2022).
[39] O. Lakhina and E. S. Swanson, Phys. Rev. D **74**, 014012 (2006).
[40] Z. G. Wang, Chin. Phys. C **48**, 103104 (2024).
[41] S. Godfrey, Phys. Rev. D **70**, 054017 (2004).
[42] E. J. Eichten, and C. Quigg, Phys. Rev. D **99**, 054025 (2019).
[43] S. C. Generalis and D. J. Broadhurst, Phys. Lett. B **139**, 85 (1984).
[44] E. Bagan, J. I. Latorre, and P. Pascual, Z. Phys. C **32**, 43 (1986).
[45] M. Karliner and J. L. Rosner, Phys. Rev. Lett. **119**, 202001 (2017).
[46] E. J. Eichten and C. Quigg, Phys. Rev. Lett. **119**, 202002 (2017).
[47] S. S. Agaev, K. Azizi, B. Barsbay, and H. Sundu, Phys. Rev. D **99**, 033002 (2019).
[48] F. S. Navarra, M. Nielsen, and S. H. Lee, Phys. Lett. B **649**, 166 (2007).
[49] R. Aaij *et al.* [LHCb Collaboration], Nature Phys. **18**, 751 (2022).
[50] R. Aaij *et al.* [LHCb Collaboration], Nature Commun. **13**, 3351 (2022).

- [51] S. S. Agaev, K. Azizi and H. Sundu, Nucl. Phys. B **975**, 115650 (2022).
- [52] S. S. Agaev, K. Azizi and H. Sundu, JHEP **06**, 057 (2022).
- [53] X. Z. Ling, M. Z. Liu, L. S. Geng, E. Wang and J. J. Xie, Phys. Lett. B **826**, 136897 (2022).
- [54] A. Feijoo, W. H. Liang and E. Oset, Phys. Rev. D **104**, 114015 (2021).
- [55] M. S. Liu, Q. F. Lu, X. H. Zhong, and Q. Zhao, Phys. Rev. D **100**, 016006 (2019).
- [56] M. G. Gordillo, F. De Soto, and J. Segovia, Phys. Rev. D **102**, 114007 (2020).
- [57] C. Deng, H. Chen, and J. Ping, from various models,” Phys. Rev. D **103**, 014001 (2021).
- [58] H. Mutuk, Phys. Lett. B **834**, 137404 (2022).
- [59] J. Zhang, J. B. Wang, G. Li, and C. S. An, Eur. Phys. J. C **82**, 1126 (2022).
- [60] H. T. An, S. Q. Luo, Z. W. Liu, and X. Liu, Eur. Phys. J. C **83**, 740 (2023).
- [61] V. O. Galkin, and E. M. Savchenko, Eur. Phys. J. A **60**, 96 (2024).